NATIONAL ADVISORY COMMITTEE FOR AERONAUTICS

TECHNICAL NOTE 2931

A METHOD FOR DETERMINING CLOUD-DROPLET IMPINGEMENT ON SWEPT WINGS

By Robert G. Dorsch and Rinaldo J. Brun

Lewis Flight Propulsion Laboratory
Cleveland, Ohio

Washington
April 1953

NATIONAL ADVISORY COMMITTEE FOR AERONAUTICS

TECHNICAL NOTE 2931

A METHOD FOR DETERMINING CLOUD-DROPLET IMPINGEMENT ON SWEPT WINGS

By Robert G. Dorsch and Rinaldo J. Brun

SUMMARY

The general effect of wing sweep on cloud-droplet trajectories about swept wings of high aspect ratio moving at subsonic speeds is discussed. A method of computing droplet trajectories about yawed cylinders and swept wings is presented, and illustrative droplet trajectories are computed.

A method of extending two-dimensional calculations of droplet impingement on nonswept wings to swept wings is presented. It is shown that the extent of impingement of cloud droplets on an airfoil surface, the total rate of collection of water, and the local rate of impingement per unit area of airfoil surface can be found for a swept wing from two-dimensional data for a nonswept wing. The impingement on a swept wing is obtained from impingement data for a nonswept airfoil section which is the same as the section in the normal plane of the swept wing by calculating all dimensionless parameters with respect to flow conditions in the normal plane of the swept wing.

INTRODUCTION

The efficient design of a thermal ice-protection system for a wing and the assessment of the heat requirements of the system necessitate a knowledge of the expected distribution of impinging supercooled cloud droplets over an airfoil surface exposed to a given set of meteorological conditions in flight. Because a closed-form solution for the equations of motion of a droplet in the flow field around an airfoil generally cannot be obtained, the impingement calculations are best performed with the aid of a differential analyzer or other computing machine. Two-dimensional calculations of droplet impingement on various airfoils, obtained with computing machines, are available in references 1 to 4. Inasmuch as reliance on such published impingement data is often necessary in the design of protective systems, an extension of the use of the available two-dimensional (nonswept) impingement data to include swept wings is desirable.

The analysis conducted at the NACA Lewis laboratory to extend the use of the two-dimensional impingement data to swept wings is presented herein.

SYMBOLS

The following symbols are used in this report:

a	droplet radius
C_D	drag coefficient for spherical droplets in air, dimensionless
d	droplet diameter
E_m	collection efficiency, dimensionless
K	inertia parameter, dimensionless
L	cylinder radius, or airfoil chord length (measured normal to leading edge)
Re	Reynolds number with respect to droplet, dimensionless
Re_0	free-stream Reynolds number, dimensionless
S	distance on surface of airfoil measured from leading-edge chord point, ratio to chord length
T	airfoil thickness, ratio to chord length
t	time
U	free-stream velocity
u	dimensionless local air velocity, ratio of local air velocity to either free-stream velocity or projection of free-stream velocity in normal plane
v	dimensionless local droplet velocity, ratio of actual droplet velocity to either free-stream velocity or projection of free-stream velocity in normal plane
W_m	rate of total impingement of water per unit span length
W_β	rate of local impingement of water in droplet form
w	liquid-water content

x,y,z	dimensionless coordinates, ratio of coordinate to either chord length or cylinder radius
α	angle of attack
β	local impingement efficiency, dimensionless
γ	angle of sweep or yaw
μ	viscosity of air
ρ_a	density of air
ρ_w	density of water
τ	time, dimensionless
ψ	scale parameter, dimensionless
ψ^*	stream function

Subscripts:

l	lower
max	maximum
n	referred to normal plane
s	referred to free-stream plane
u	upper
x	component in x-direction
y	component in y-direction
z	component in z-direction

ANALYSIS

Flow Field

A knowledge of the flow field about a swept wing is required in the droplet-impingement calculations, because the motion of a droplet is governed by the momentum of the droplet and by the drag forces

imposed on the droplet by the relative motion between the droplet and the air which is moving along the streamlines around the wing. The droplet momentum tends to keep the droplet moving in a straight path, while the drag forces tend to force the droplet to follow the streamlines.

Because of its geometric and aerodynamic simplicity, the problem of impingement on a yawed circular cylinder will be considered first. The method developed for the cylinder will apply equally well to a swept wing, and this application will be discussed in detail in a subsequent section.

The incompressible nonviscous velocity field around a yawed circular cylinder of infinite span can be divided into components in the x-, y-, and z-directions, as shown in figure 1. The right-rectangular coordinate system is established so that the center line of the cylinder coincides with the z-axis. The angle of yaw γ is measured with respect to the negative x-axis. The flow in the xy-plane (normal plane) is the same as the flow about a nonyawed circular cylinder which has a free-stream velocity equal to the component of the free-stream velocity in the normal plane $U_s \cos \gamma$. The velocity component in the z-direction is a constant throughout the flow field, and the magnitude of the component is determined by the projection of the free-stream velocity on the z-axis $U_s \sin \gamma$.

The effect of yaw on the streamlines and local air velocity vectors can be illustrated by an example in which the flow field about a yawed circular cylinder is presented. For this example, the yawed cylinder is assumed oriented in an x,y,z-coordinate system as shown in figure 1. The angle of yaw γ with respect to the free-stream direction is 30°. The projection of two streamlines, selected for illustration, upon the xy- and xz-planes is shown in figure 2. (The method of calculation is given in appendix A.) Also shown are the projections of velocity vectors upon the xz-plane at various points in the sheet (surface perpendicular to the xy-plane containing the streamline) which contains each streamline. Considerable deviation of the streamlines from the projection of the free-stream direction in the xz-plane is indicated in the figure. The curvature of the streamlines in the xz-plane is due to the fact that, whereas the u_x component changes in magnitude with x and y, u_z is a constant independent of x or y. The z velocity component u_z is a constant throughout the flow field, because in a frictionless fluid it is equal only to the projection along the z-axis of the free-stream velocity U_s and is not influenced by the perturbation velocity of the cylinder in the xy-plane. The maximum curvature of the streamline projections in the xz-plane takes place in those

streamlines located near a surface defined by the stagnation streamlines. This maximum curvature of the stagnation streamlines is to be expected, because along a stagnation line where u_x becomes small (close to the body), u_z is relatively predominant and the displacement is primarily in the z-direction.

Method of Calculating Droplet Trajectories

Inasmuch as the projection of the path of an air particle in the xz-plane does not remain in the free-stream direction but rather is a curved path, the projected path of the droplets in the xz-plane will also be curved. Because of inertia, the droplets will be deflected less from the free-stream direction than will the air. The dimensionless equations that describe the motion of droplets along a trajectory in a three-dimensional flow field can be written in terms of the x-, y-, and z-components as follows (refs. 5 and 6):

$$\frac{dv_x}{d\tau} = \frac{C_D Re}{24} \frac{1}{K} (u_x - v_x) \tag{1a}$$

$$\frac{dv_y}{d\tau} = \frac{C_D Re}{24} \frac{1}{K} (u_y - v_y) \tag{1b}$$

$$\frac{dv_z}{d\tau} = \frac{C_D Re}{24} \frac{1}{K} (u_z - v_z) \tag{1c}$$

where

$$\tau = \frac{tU_s}{L}$$

and

$$K = \frac{2}{9} \frac{\rho_w a^2 U_s}{\mu L} \tag{2}$$

The Reynolds number Re with respect to the droplet is obtained from the following relation:

$$\left(\frac{Re}{Re_{0,s}}\right)^2 = (u_x - v_x)^2 + (u_y - v_y)^2 + (u_z - v_z)^2 \tag{3}$$

where

$$Re_{0,s} = \frac{2a\rho_a U_s}{\mu} \tag{4}$$

The coefficient of drag C_D is a function of Re. The values of C_D corresponding to various values of Re are obtained from experimental drag data (ref. 7).

The solution of equation (1) to obtain three-dimensional droplet trajectories about a yawed cylinder of infinite span is not very much more difficult than the two-dimensional solution for the nonyawed cylinder, because the air velocity components u_x and u_y are independent of z and because the droplet and air velocity components in the z-direction are equal. Because $v_z = u_z$, there is no z-component of drag, and equation (1c) reduces to:

$$\frac{dv_z}{d\tau} = 0$$

and

$$z = u_z\tau + \text{constant} \tag{5}$$

Furthermore, equation (3) reduces to

$$\left(\frac{Re}{Re_{0,s}}\right)^2 = (u_x - v_x)^2 + (u_y - v_y)^2 \tag{6}$$

Because of the properties of the flow field discussed in the preceding paragraph, the projection of the droplet trajectories on the xy-plane can be obtained by the simultaneous solution of equations (1a) and (1b) with the aid of a differential analyzer. The manner of calculating is the same as the two-dimensional method presented in reference 6, if the component of the free-stream velocity in the normal plane is used throughout the computations instead of the free-stream velocity U_s. In order to perform this calculation, both sides of equations (1) and (6) are divided by $\cos^2\gamma$. Thus, all velocities are used in the form of a ratio to the normal component of the free-stream velocity; τ becomes $\tau_n = tU_n/L$; and equations (2), (4), and (6) become

$$K_n = \frac{2}{9}\frac{\rho_w a^2 U_s \cos\gamma}{\mu L} \equiv \frac{2}{9}\frac{\rho_w a^2 U_n}{\mu L} \tag{7}$$

$$Re_{0,n} = \frac{2a\rho_a U_s \cos\gamma}{\mu} \equiv \frac{2a\rho_a U_n}{\mu} \tag{8}$$

and

$$\left(\frac{Re}{Re_{0,n}}\right)^2 = (u_{x,n} - v_{x,n})^2 + (u_{y,n} - v_{y,n})^2 \tag{9}$$

respectively. The dimensionless equations of the x- and y-components of motion of the droplet along a trajectory are now in a form identical to that of the equations for a nonyawed cylinder. In addition, the x- and y-components of the velocity field about a yawed cylinder will be in a dimensionless form identical to that of the x- and y-components for a nonyawed cylinder (appendix A).

The projection of the droplet trajectories upon the xz-plane is obtained by the simultaneous solution of equations (1a) and (5), which is accomplished if the relation between x and τ_n is known. This relation between x and τ_n can be obtained from a differential analyzer as it solves the xy-component of the trajectories. The value of z corresponding to the various values of x can be obtained from equation (5), where $u_{z,n} = v_{z,n} = \tan \gamma$ (appendix A).

Sample Droplet Trajectories About Yawed Cylinder

Three-dimensional droplet trajectories were calculated for a yawed cylinder for conditions where the inertia parameter K_n is equal to 2.78 and the free-stream Reynolds number in the normal plane $Re_{0,n}$ is equal to 100. The projections upon the xy- and xz-planes of typical droplet trajectories are shown in figure 3. The starting ordinate (at $x = -\infty$) in the xy-plane for each trajectory is given by the value of y_0 in the figure.

Swept Wings

The calculation of droplet trajectories about a swept wing can be accomplished by the method used for the yawed cylinder in the preceding sections, if the flow field about a swept wing is approximated (except near the fuselage and wing tips) by the incompressible nonviscous flow about an infinite-span wing of zero taper at an angle of yaw equal to the sweep angle. This approximation is valid for wings of high aspect ratio and small taper.

The nonviscous flow field about a yawed wing of infinite span can be obtained in the same manner as that for the yawed cylinder by determining the components in the normal (xy) plane (fig. 4) and the component parallel to the leading edge (z-direction). The flow field in the normal plane is determined from two-dimensional theory by using the airfoil section in the normal plane and the component of the free-stream velocity in the normal plane $U_s \cos \gamma$. As before, the z-component is constant throughout the flow field, being simply the projection of the free-stream velocity upon the z-axis $U_s \sin \gamma$.

When the swept wing is at a free-stream angle of attack α_s (fig. 4), the effective angle of attack in the normal plane, to a close approximation, is $\alpha_n = \alpha_s \sec \Upsilon$ and the components of the free-stream velocity are $U_s \sin \Upsilon_\alpha$ and $U_s \cos \Upsilon_\alpha$, where Υ_α is the angle between U_s and U_n. For small angles of attack, Υ_α is for all practical purposes equal to Υ and therefore Υ can be used when calculating the components of the free-stream velocity; however, the corrected angle of attack $\alpha_s \sec \Upsilon$ must be used in obtaining the flow field in the normal plane.

Air streamlines about a 65_1-212 airfoil at 45° yaw and an angle of attack in the normal plane of 4° ($\alpha_s = 2.8°$) are shown in figure 5. The projection of three streamlines on the xy-plane from $x = -1$ to 0.1 is shown in figure 5(a), and the projection on the xz-plane is shown in figure 5(b). The method used to obtain the streamlines is given in appendix B. As for the cylinder, the projections of the streamlines in the xz-plane deviate from the projection of the free-stream direction because of changes in u_x. The deviation from the projection of the free-stream direction is considerably less for the airfoil than for a cylinder with the same chord length, as would be expected from comparison of the velocity field of a thin body with that of a blunt body.

Sample Droplet Trajectories About Yawed Wing

The projections upon the xy- and xz-planes of typical droplet trajectories about a 65_1-212 airfoil with $\alpha_s = 2.8°$ ($\alpha_n = 4°$) and at a yaw angle of 45° are shown in figure 5 for values of $K_n = 0.1$ and $Re_{0,n} = 128$. As in the case of the air streamlines, there is less curvature of the xz-projection of the trajectory for the airfoil than for the relatively blunt cylinder. For example, up to about 1 chord length ($x = -1$, fig. 5(b)) ahead of the wing the droplets are essentially undeviated from the free-stream plane; whereas, for the cylinder they are undeviated only up to about 2 diameters ($x = -5$, fig. 3) ahead of the cylinder.

RESULTS AND DISCUSSION

It was shown in the ANALYSIS that the equations of the x- and y-components of motion of the droplet trajectories and of the air-velocity field around a swept wing can be put in the same dimensionless form as the x- and y-components of motion for the two-dimensional (nonswept) case. Because of the identical form of the dimensionless equations, it is possible to obtain the xy-projection of the droplet trajectories around a swept wing from two-dimensional trajectory data

by using the component of the free-stream velocity in the normal plane and the angle of attack in the normal plane corresponding to the given angle of sweep Υ when evaluating the various dimensionless parameters. The projection of the trajectories in the xz-plane cannot be obtained from two-dimensional data without recalculation with a differential analyzer. A knowledge of the projection of the trajectories in the xz-plane is not usually needed in order to obtain an appraisal of the impingement of droplets on a swept wing, because the motion of the droplets in the xz-plane does not influence the chordwise droplet-impingement distribution calculated from trajectories in the xy-plane. The spanwise displacement of the droplets does cause a small spanwise shift in the point of impingement. For droplets of uniform size, the xy-impingement pattern is thus displaced spanwise a small amount; but as the trajectories in the xy-plane are not dependent on z, the impingement distribution on an airfoil section in the normal plane is the same at all spanwise (z) positions along the wing. If the cloud consists of droplets having a distribution of droplet sizes, each size will be shifted spanwise a slightly different amount; but the net chordwise impingement in the normal plane at each spanwise station will be the same as the net impingement calculated from the xy-component of the trajectories when the given droplet-size distribution is used.

Example of application of two-dimensional data to swept wing. - The determination of droplet impingement on a swept wing from two-dimensional data calculated for nonswept wings, such as presented in references 1 to 4, is best illustrated with an example.

For the example, a wing with a 65_1-212 airfoil section in the normal plane is swept to an angle of 45°. The chord length in the normal plane is $8\frac{1}{3}$ feet, and the free-stream angle of attack is 2.8° ($\alpha_n = 4^\circ$). The swept wing is assumed to be moving in the free-stream direction at 525 miles per hour through a cloud composed of droplets all of which are 20 microns in diameter; the liquid-water content of the cloud is assumed to be 0.2 gram per cubic meter; and the free-air temperature is -11° F at a pressure altitude of 20,000 feet.

The extent of impingement on the airfoil, the rate of collection of total water, and the rate of impingement per unit area of airfoil surface can be found for this swept wing from two-dimensional data for an NACA 65_1-212 nonswept wing presented in reference 2, provided the values of the dimensionless parameters required for entering the data figures of reference 2 are calculated for the normal plane. The required dimensionless parameters K_n, ψ_n, and $Re_{0,n}$ for the swept wing are

$$U_n = U_s \cos \gamma = 371 \text{ mph}$$

$$K_n = 1.704 \times 10^{-12} \frac{d^2 U_n}{\mu L} = 0.09$$

$$Re_{0,n} = 4.813 \times 10^{-6} \frac{d \rho_a U_n}{\mu} = 131$$

and

$$\psi_n = \frac{Re_{0,n}}{K_n} = 1455$$

(Factors required for converting from self-consistent units required in eqs. (1) to (9) to units most commonly used in aeronautics are given in ref. 2.) Typical droplet trajectories which approximately correspond to these values of K_n and $Re_{0,n}$ are given in figure 5. From the method of reference 2, the farthest point of impingement on the upper surface S_u of the airfoil obtained from figure 6(a) ($\psi = \psi_n$ and $Re_0 = Re_{0,n}$) is 0.025 chord length, and the farthest point of impingement on the lower surface S_l (fig. 6(b)) is 0.14. The collection efficiency E_m corresponding to these values of $Re_{0,n}$ and ψ_n is 0.24 (fig. 7). The rate of total water in droplet form impinging on the swept wing in pounds per hour per unit span (parallel to the leading edge) is

$$W_m = 0.329 E_m T U_s w \cos \gamma = 5.86 \text{ lb/(hr)(ft span)}$$

The term $\cos \gamma$ is introduced into the equation to account for the increased spanwise length of wing sweeping out a given volume of cloud in comparison with an identical nonswept wing moving with the same free-stream velocity. That is, the water collection rate per unit span is reduced by $\cos \gamma$ for the swept wing, which is consistent with the mathematical artifice of considering the airfoil to be moving forward in the normal direction with a velocity $U_s \cos \gamma$.

The maximum local impingement efficiency factor β_{max} obtained from figure 8 is 0.55, which occurs at 0.008 chord length along the lower surface. The location of the region of maximum local impingement is of importance when determining the most effective location of the parting strip on a cyclical thermal de-icing system. The maximum rate of local impingement is

$$W_{\beta,max} = 0.329 U_s w \beta_{max} \cos \alpha_n \cos \gamma = 13.39 \text{ lb/(hr)(sq ft)}$$

Similar calculations for an identical nonyawed wing moving at the same free-stream velocity (525 mph) in an identical environment (d, 20 microns; w, 0.2 g/cu m; temperature, -11° F at 20,000 ft pressure altitude) give the farthest point of impingement on the upper surface as 0.028 chord length and the farthest point of impingement on the lower surface as 0.17 chord length, the collection efficiency E_m equal to 0.28, the total water catch as 9.67 pounds per hour per foot span, the maximum local impingement efficiency β_{max} equal to 0.58, and the maximum rate of local impingement $W_{\beta,max}$ equal to 19.98 pounds per hour per square foot. (For purposes of comparison, the assumption has been made in this paragraph that the impingement data of reference 2 are valid beyond the critical Mach number of the nonswept wing, which may not be true.)

The method for obtaining the impingement on a swept wing was derived for a wing of zero taper. The calculations for a wing with small taper can be made from the impingement data in the same manner as suggested in reference 2 for nonswept wings with small taper.

The impingement on a yawed cylinder can be obtained from two-dimensional data by a procedure similar to that illustrated for the swept wing. The pertinent dimensionless parameters, conversion factors, and practical units for the circular cylinder are given in reference 6.

Transformation of airfoil section from free-stream plane to normal plane. - The method discussed for obtaining impingement on a swept wing from two-dimensional data requires a knowledge of the airfoil section in the normal plane. If a swept-wing layout has its design airfoil section in the free-stream plane rather than in the normal plane, then it is necessary to determine the airfoil section in the normal plane. This transformation can be made by multiplying the airfoil ordinates by the secant of the sweep angle. Thus, the airfoil section found for the normal plane will have a thickness ratio which is larger by the factor $\sec \gamma$. For example, at 40° sweep angle a wing with a 6-percent-thick airfoil section in the free-stream plane will have approximately an 8-percent-thick (7.83) airfoil section in the normal plane. In addition, for most airfoil types the section in the normal plane will be, to a satisfactory approximation, a member of the same airfoil family as the airfoil section in the free-stream plane. Noncambered airfoils generally transform in this manner so as to correspond more closely to a member in the same family than do those with appreciable camber.

Value of xz-projection of droplet trajectories. - Although the projections of the droplet trajectories upon the xz-plane are not needed for determining droplet impingement upon a swept wing, a knowledge of the xz-projection is of value when considering the impingement of droplets on small wing appendages. This knowledge is particularly useful when considering the impingement on appendages located near the leading edge of a swept wing, such as boom-mounted pressure-sensing elements, wing

fences, and small leading-edge inlets. Although these devices will change the local flow field to some extent, the impingement zone would generally be expected to extend farther back on the inboard side of protuberances and on the outboard side of cavities than on the opposite or "shadowed" side of the appendages attached to a sweptback wing. For appendages attached to a sweptforward wing the same thing would occur, except that "outboard" and "inboard" should be interchanged in the preceding sentence.

Application to supersonic velocities. - The preceding sections have specifically treated only the extension of droplet-impingement data for nonswept wings to swept wings moving at subsonic velocities in an incompressible fluid. The same general approach can be employed to obtain impingement data for swept wings of high aspect ratio moving at supersonic speeds from nonswept-wing impingement data calculated for supersonic velocities in a compressible fluid. This extension is possible because, irrespective of the magnitude of the velocity, the component of translation of any cylindrical body in the direction of its long axis has no effect on the motion of a frictionless fluid. The flow around a wing of constant section moving through a fluid at rest is determined by the normal components of velocity of its solid boundaries, and these components in turn are completely specified by the component of motion in planes perpendicular to the axis $U_S \cos \Upsilon$ (ref. 8). Thus, the impingement on a swept wing of high aspect ratio moving at supersonic velocity can be determined from two-dimensional (nonswept-wing) data calculated for a wing with the same airfoil section as the normal airfoil section of the swept wing and moving through an identical environment at a Mach number equal to the Mach number found for the normal plane of the swept wing.

2751

CONCLUSIONS

An analysis of the general effect of sweep on the droplet trajectories about a swept airfoil and a method of calculating the droplet trajectories have been presented. The extent of impingement of cloud droplets on the airfoil surface, the rate of collection of total water in droplet form, and the local rate of impingement per unit area of the airfoil surface can be found for a swept wing from two-dimensional data for a nonswept wing with the same airfoil section as the section in the normal plane of the swept wing. The values of the dimensionless parameters required in order to interpret the two-dimensional data are calculated with respect to the normal plane of the swept wing rather than with respect to the free-stream plane as is the usual procedure for nonswept wings.

Lewis Flight Propulsion Laboratory
National Advisory Committee for Aeronautics
Cleveland, Ohio, February 12, 1953

APPENDIX A

CALCULATION OF STREAMLINES AND VELOCITY VECTORS ABOUT CIRCULAR CYLINDER AT YAW ANGLE γ

A cylinder oriented with the axis along the z-axis of an x,y,z-cartesian coordinate system (fig. 1) is considered for the three-dimensional derivation of the velocity field around a yawed cylinder. The stream function for nonviscous incompressible flow in the x'y'-plane using polar coordinates r' and θ and letting $\psi^* = 0$ at the surface of the cylinder is

$$\psi^* = U_n \left(r' - \frac{L^2}{r'}\right) \sin \theta \tag{A1}$$

where L is the radius of the cylinder, and the terms with the prime superscript have the dimensions of length. Or, in dimensionless form

$$\frac{\psi^*}{U_n L} = \left(r - \frac{1}{r}\right) \sin \theta \tag{A2}$$

where $(r = r'/L)$ and $\psi^*/U_n L$ are dimensionless. For various $\psi^*/U_n L$ values, the x- and y-coordinates (x and y are dimensionless), which can be obtained from equation (A2), give the projection of the streamline upon the xy-plane.

The projection of the streamline in the xz-plane can be obtained as follows: The streamlines in the xy-plane are divided into small line segments. The x-component of velocity corresponding to the i^{th} segment is determined from the average of the velocities determined by the x and y values of the end points of the i^{th} segment. The time required for an air particle to travel the i^{th} segment of a trajectory is

$$(\Delta\tau_n)_i = \frac{\Delta x_i}{(u_{x,n})_i}$$

The displacement in the z-direction while the air particle travels a distance Δx_i in the x-direction is

$$\Delta z_i = (\Delta\tau_n)_i \, (u_{z,n})_i$$

From any arbitrary point ahead of the cylinder, for each x_i

$$z_i = \sum_0^i (\Delta\tau_n)_i \, (u_{z,n})_i = u_{z,n} \sum_0^i (\Delta\tau_n)_i$$

since $u_{z,n}$ is constant.

The dimensionless velocity components of the flow field about a circular cylinder at yaw angle γ are

$$u_{x,n} = \frac{u_x^i}{U_s \cos\gamma} = \left[1 - \frac{x^2 - y^2}{(x^2 + y^2)^2}\right]$$

$$u_{y,n} = \frac{u_y^i}{U_s \cos\gamma} = -\left[\frac{2xy}{(x^2 + y^2)^2}\right]$$

$$u_{z,n} = \frac{u_z^i}{U_s \cos\gamma} = \frac{U_s \sin\gamma}{U_s \cos\gamma} = \tan\gamma$$

where the velocity components with the prime superscript have the usual dimensions associated with velocity.

Projections upon the xy-plane of streamlines about a 30°-yawed cylinder for $\psi^*/U_nL = 0.19$ and $\psi^*/U_nL \to 0$ (infinitesimally greater than zero) are shown in figure 2(a). The corresponding projections upon the xz-plane along with the projections in the xz-plane of the velocity vectors in the sheets containing the selected streamlines are shown in figure 2(b).

APPENDIX B

CALCULATION OF STREAMLINES AND VELOCITY VECTORS ABOUT WING WITH 65_1-212 AIRFOIL AT YAW ANGLE γ AND ANGLE OF ATTACK α_s

For a wing in an x,y,z-coordinate system with its leading edge along the z-axis and the free-stream direction at an angle γ with the negative x-axis (fig. 4), the equations of the velocity components of the air flow about the wing can be written (by using the vortex method of ref. 2 and summing the contributions of 300 vortex elements distributed on both the upper and lower surfaces of the airfoil)

$$u'_x = U_s \cos\gamma \sum_{i=0}^{300} \frac{u_s(y-\eta)}{2\pi r^2} \Delta S + U_s \cos\gamma \cos\alpha_n$$

$$u'_y = U_s \cos\gamma \sum_{i=0}^{300} \frac{u_s(\xi-x)}{2\pi r^2} \Delta S + U_s \cos\gamma \sin\alpha_n$$

$$u'_z = U_s \sin\gamma$$

where ξ and η are dimensionless coordinate points (ratio to chord length) on the airfoil, r is the distance (ratio to chord length) from an element of the vortex sheet to a point in the flow field, S is the distance (ratio to chord length) from chord line measured along the surface of the airfoil, the subscript S refers to the airfoil surface, and the prime superscript indicates that a term has the usual dimensions.

Dividing both sides by the normal velocity component yields

$$u_{x,n} = \frac{u'_x}{U_s \cos\gamma} = \frac{u'_x}{U_n} = \sum_{i=0}^{300} \frac{u_s(y-\eta)}{2\pi r^2} \Delta S + \cos\alpha_n$$

$$u_{y,n} = \frac{u'_y}{U_s \cos \gamma} = \frac{u'_y}{U_n} = \sum_{i=0}^{300} \frac{u_s(\xi - x)}{2\pi r^2} \Delta S + \sin \alpha_n$$

$$u_{z,n} = \frac{u'_z}{U_s \cos \gamma} = \frac{u'_z}{U_n} = \tan \gamma$$

The summation terms in the equations were computed with the aid of a punched-card electronic calculating machine (ref. 2).

Inasmuch as a closed-form solution of the equation of the streamlines was not available, the streamlines were obtained by a simultaneous solution of the following equations with the aid of the differential analyzer:

$$x = x_0 + \int u_{x,n} \, d\tau_n$$

$$y = y_0 + \int u_{y,n} \, d\tau_n$$

$$z = z_0 + u_{z,n} \, \tau_n$$

where the subscript 0 refers to the starting coordinate.

The projections of the streamlines in the xy- and xz-planes for a 65_1-212 airfoil at a normal angle of attack of 4° ($\alpha_s = 2.8^\circ$) and 45° angle of yaw are shown in figure 5.

REFERENCES

1. Guibert, A. G., Janssen E., and Robbins, W. M.: Determination of Rate, Area, and Distribution of Impingement of Waterdrops on Various Airfoils from Trajectories Obtained on the Differential Analyzer. NACA RM 9A05, 1949.

2. Brun, Rinaldo J., Serafini, John S., and Moshos, George J.: Impingement of Water Droplets on an NACA 65_1-212 Airfoil at an Angle of Attack of 4°. NACA RM E52B12, 1952.

3. Lenherr, F. E., and Thomson, J. E.: Preliminary Report on the Computation of Water Drop Trajectories about a 6 Percent Airfoil. TDM 67, Northrop Aircraft, Inc., Aug. 14, 1952.

4. Bergrun, Norman R.: An Empirical Method Permitting Rapid Determination of the Area, Rate, and Distribution of Water-Drop Impingement on an Airfoil of Arbitrary Section at Subsonic Speeds. NACA TN 2476, 1951.

2751

5. Langmuir, Irving, and Blodgett, Katherine B.: A Mathematical Investigation of Water Droplet Trajectories. Tech. Rep. No. 5418, Air Materiel Command, AAF, Feb. 19, 1946. (Contract No. W-33-038-ac-9151 with General Electric Co.)

6. Brun, Rinaldo J., and Mergler, Harry W.: The Impingement of Water Droplets on a Cylinder in an Incompressible Flow Field and Evaluation of Rotating Multicylinder Method for Measurement of Droplet-Size Distribution, Volume-Median Droplet Size, and Liquid-Water Content in Clouds. NACA TN 2904, 1953.

7. Wien, W., and Harms, F., eds.: Handbuch der Experimentalphysik. Teil 4, Bd. 4, Akademische Verdagsgesellschaft M.B.H. (Leipzig), 1932.

8. Jones, Robert T.: Wing Plan Forms for High-Speed Flight. NACA Rep. 863, 1947. (Supersedes NACA TN 1033.)

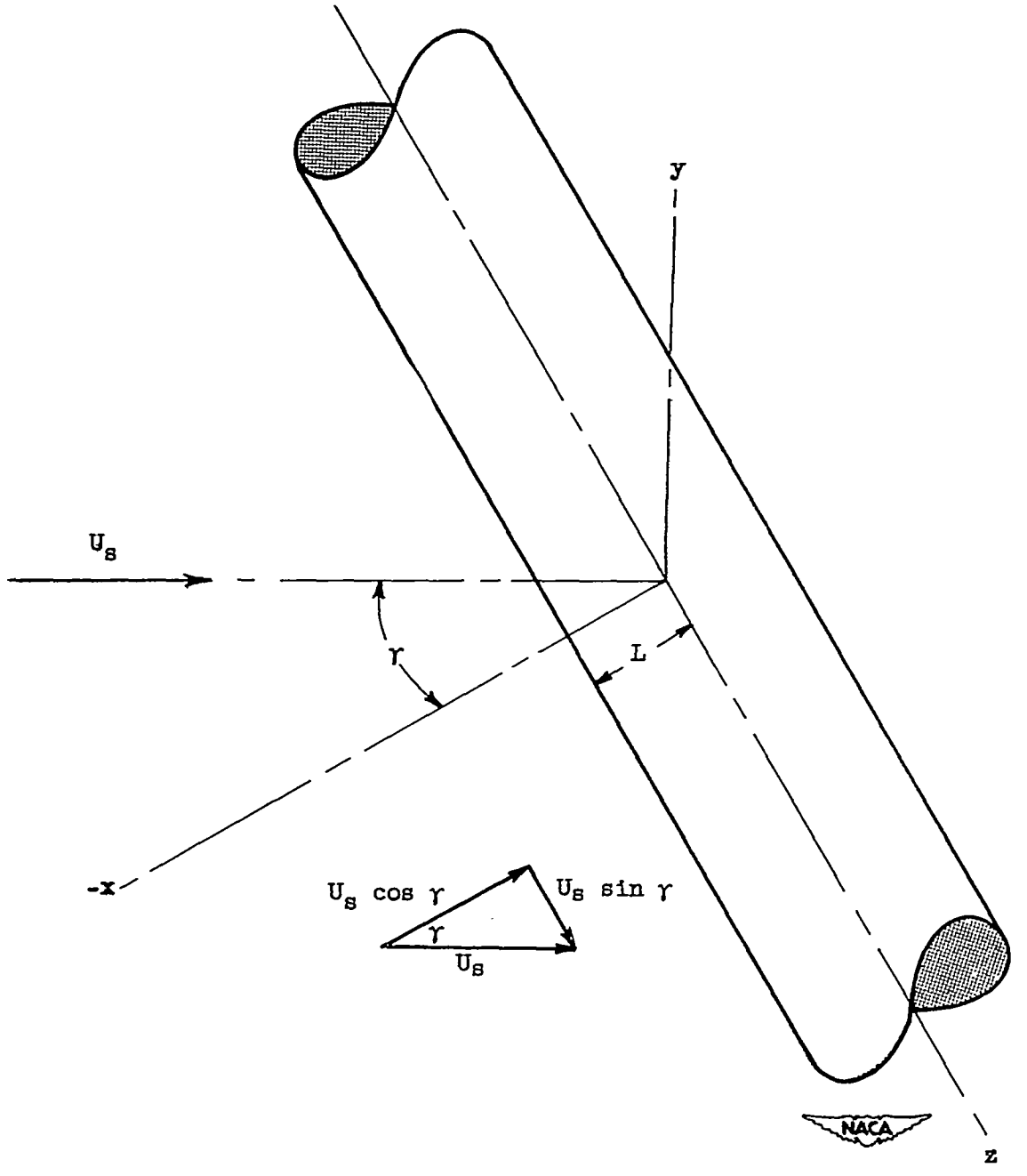

Figure 1. - Coordinate system for circular cylinder at yaw angle γ.

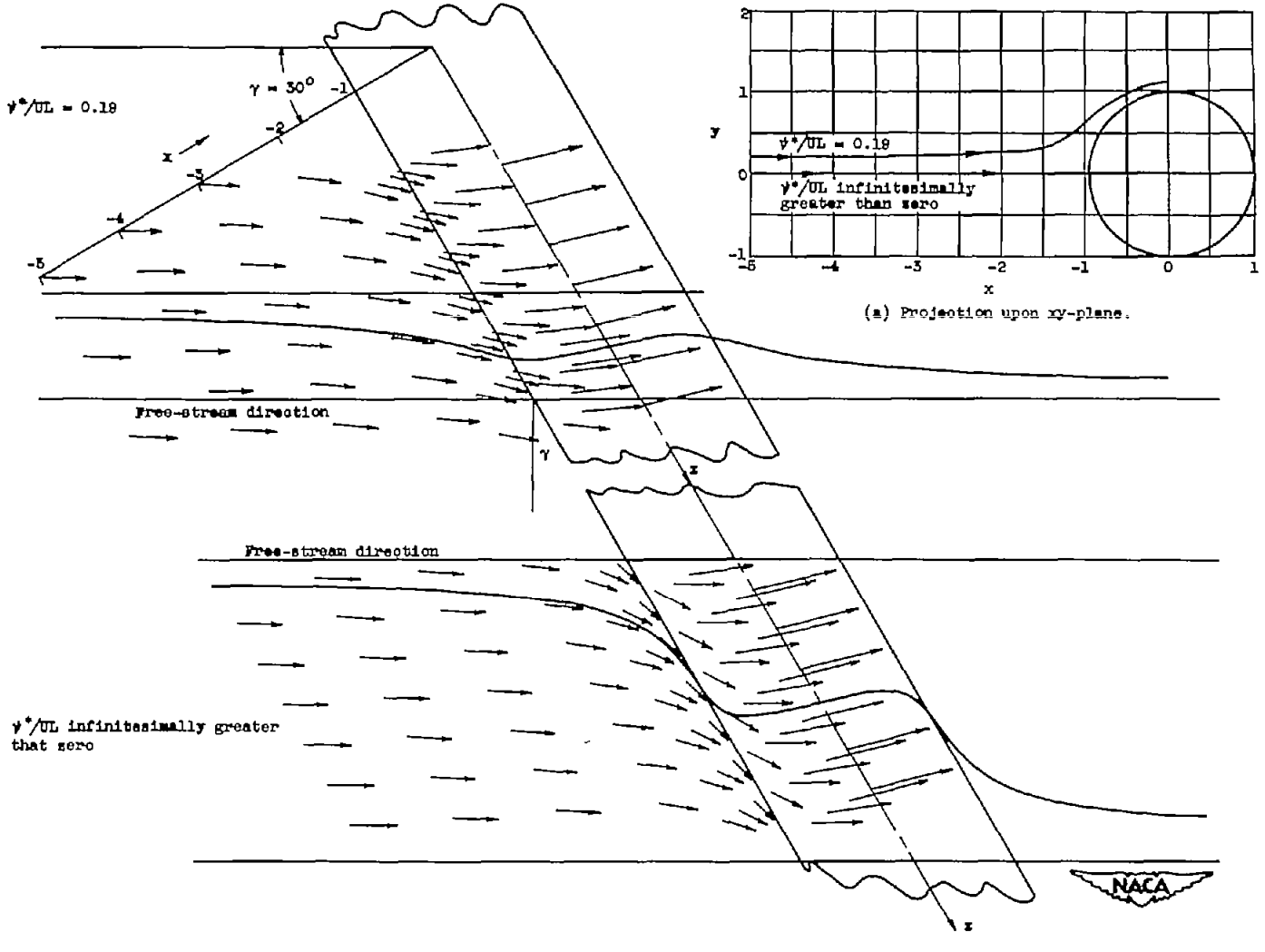

(a) Projection upon xy-plane.

(b) Projection upon xz-plane. (Arrows represent xz-component of local air velocities in each sheet.)

Figure 2. - Streamlines around 30°-yawed circular cylinder.

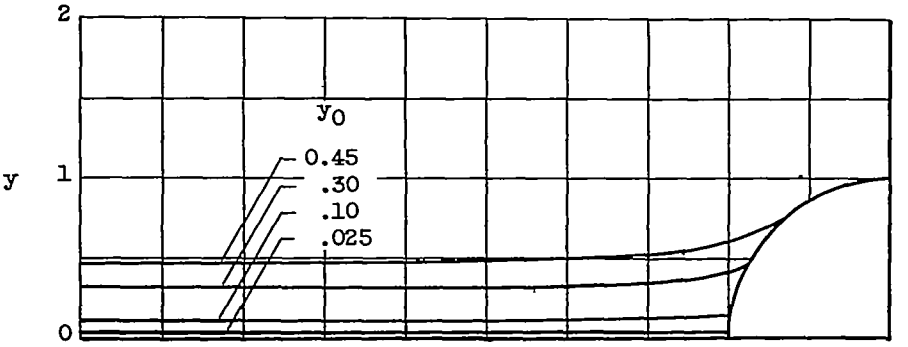

(a) Projection upon xy-plane.

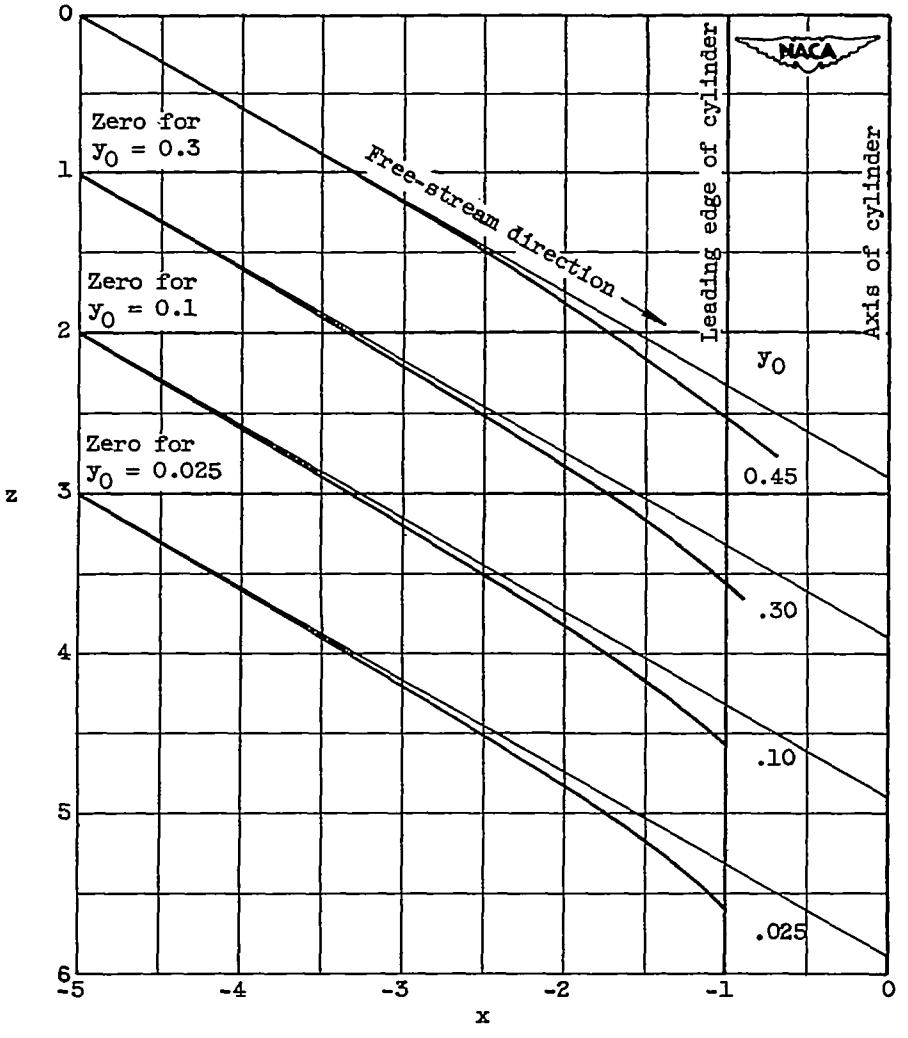

(b) Projection upon xz-plane.

Figure 3. - Droplet trajectories in vicinity of circular cylinder at 30° yaw. Inertia parameter K_n, 2.78; free-stream Reynolds number $Re_{0,n}$, 100.

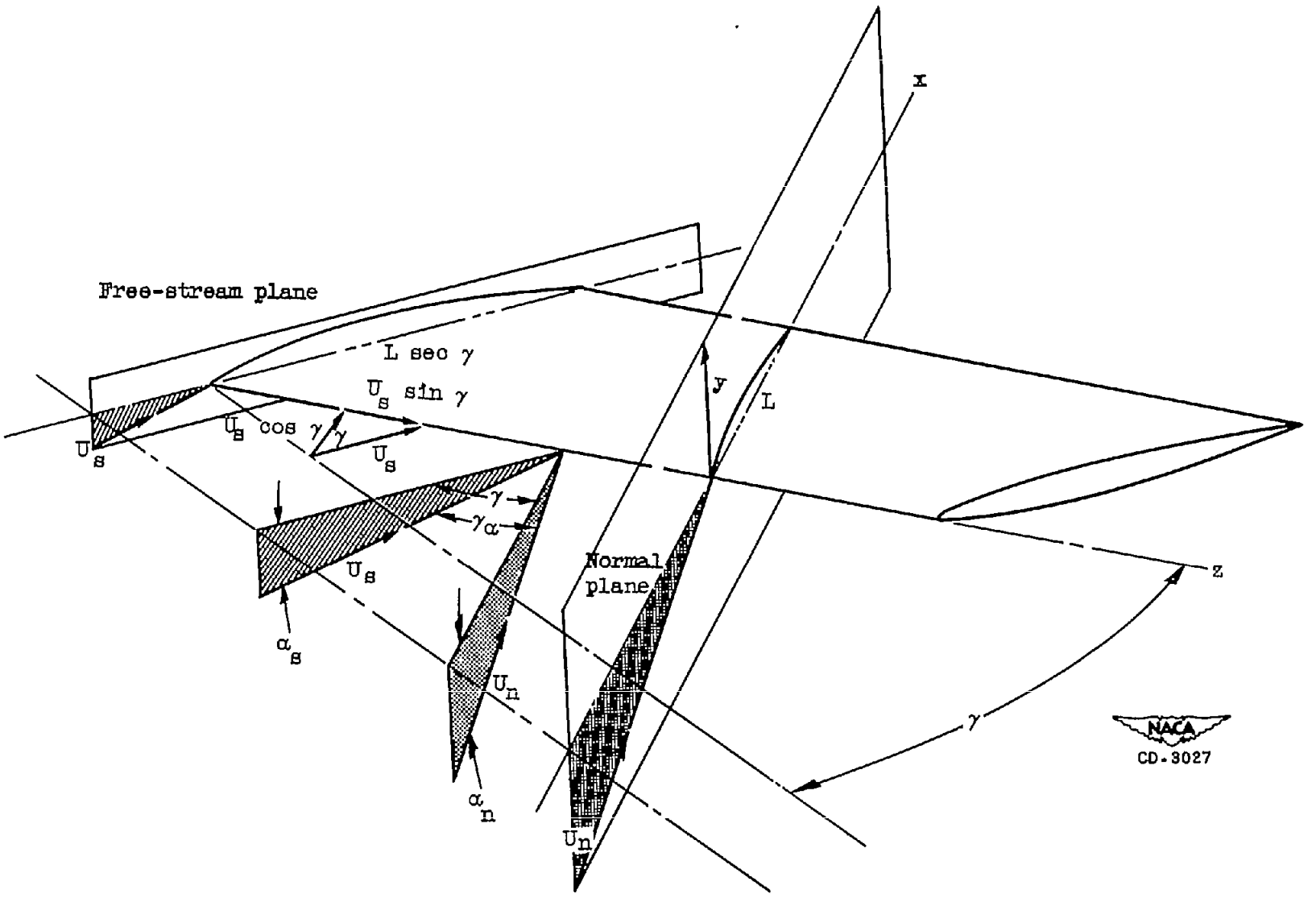

Figure 4. - Geometry applicable to yawed wing.

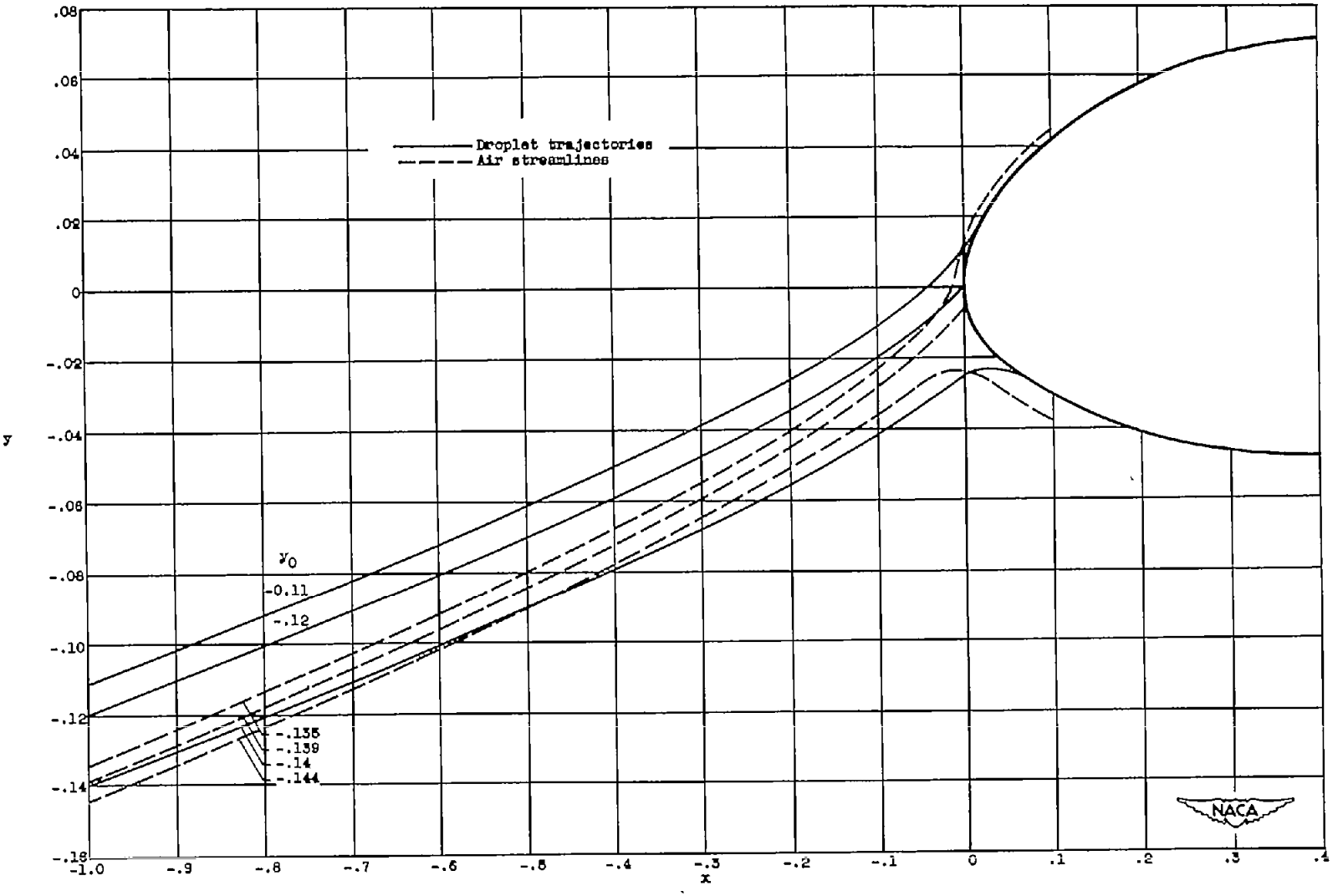

(a) Projection upon xy-plane. (Ordinate scale expanded x4.)

Figure 6. - Typical air streamlines and water-droplet trajectories in the vicinity of 65_1-212 airfoil at yaw angle of 45°. Angle of attack α_n, 4°; inertia parameter K_n, 0.1; free-stream Reynolds number $Re_{0,n}$, 128.

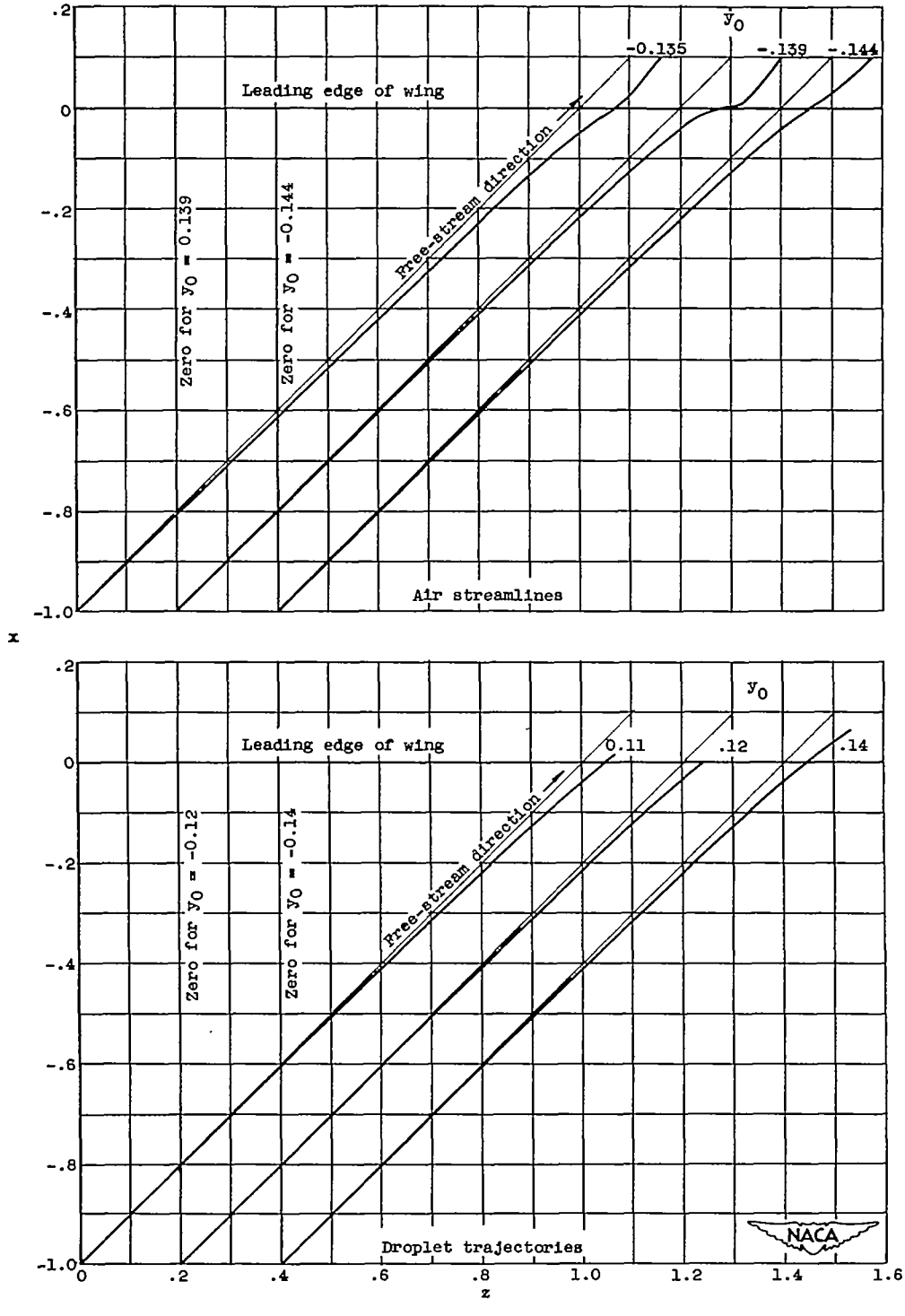

(b) Projection upon xz-plane.

Figure 5. - Concluded. Typical air streamlines and water-droplet trajectories in the vicinity of 65_1-212 airfoil at yaw angle of 45°. Angle of attack α_n, 4°; inertia parameter K_n, 0.1; free-stream Reynolds number $Re_{0,n}$, 128.

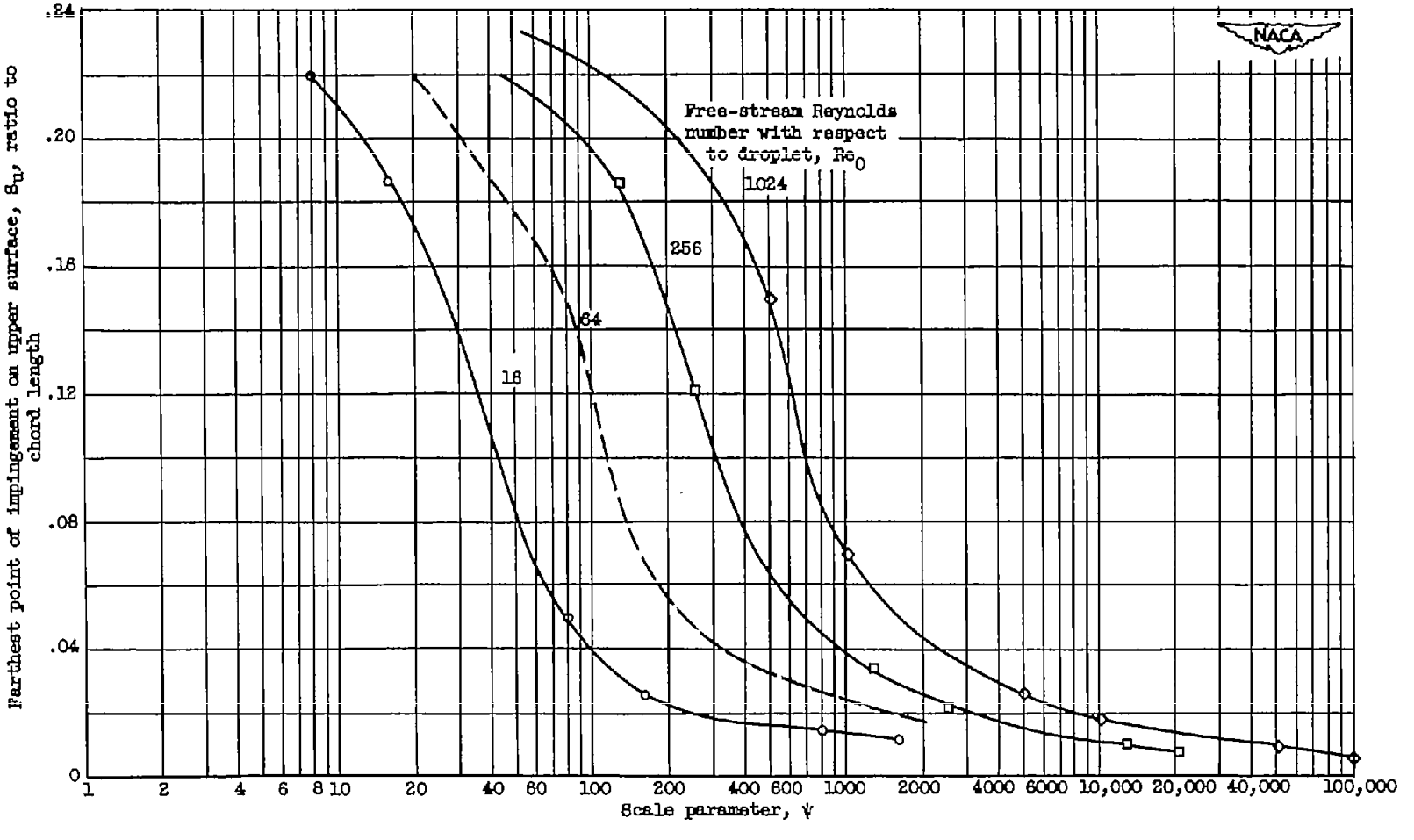

(a) Upper surface.

Figure 6. - Farthest point of droplet impingement on airfoil surface. NACA 65_1-212 airfoil; angle of attack, 4°. (Reproduced from fig. 6, ref. 2.)

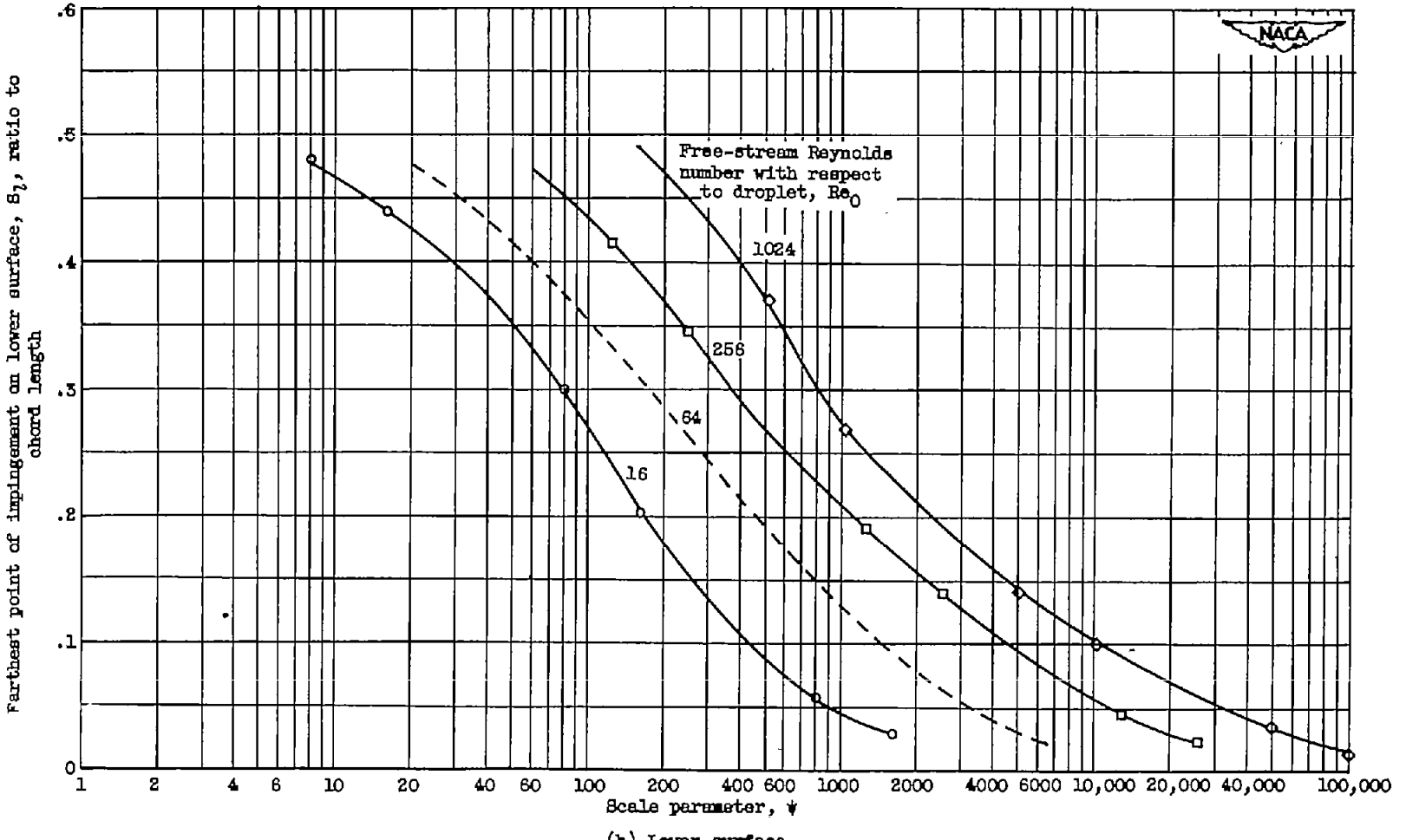

(b) Lower surface.

Figure 6. - Concluded. Farthest point of droplet impingement on airfoil surface. NACA 65_1-212 airfoil; angle of attack, 4°. (Reproduced from fig. 6, ref. 2.)

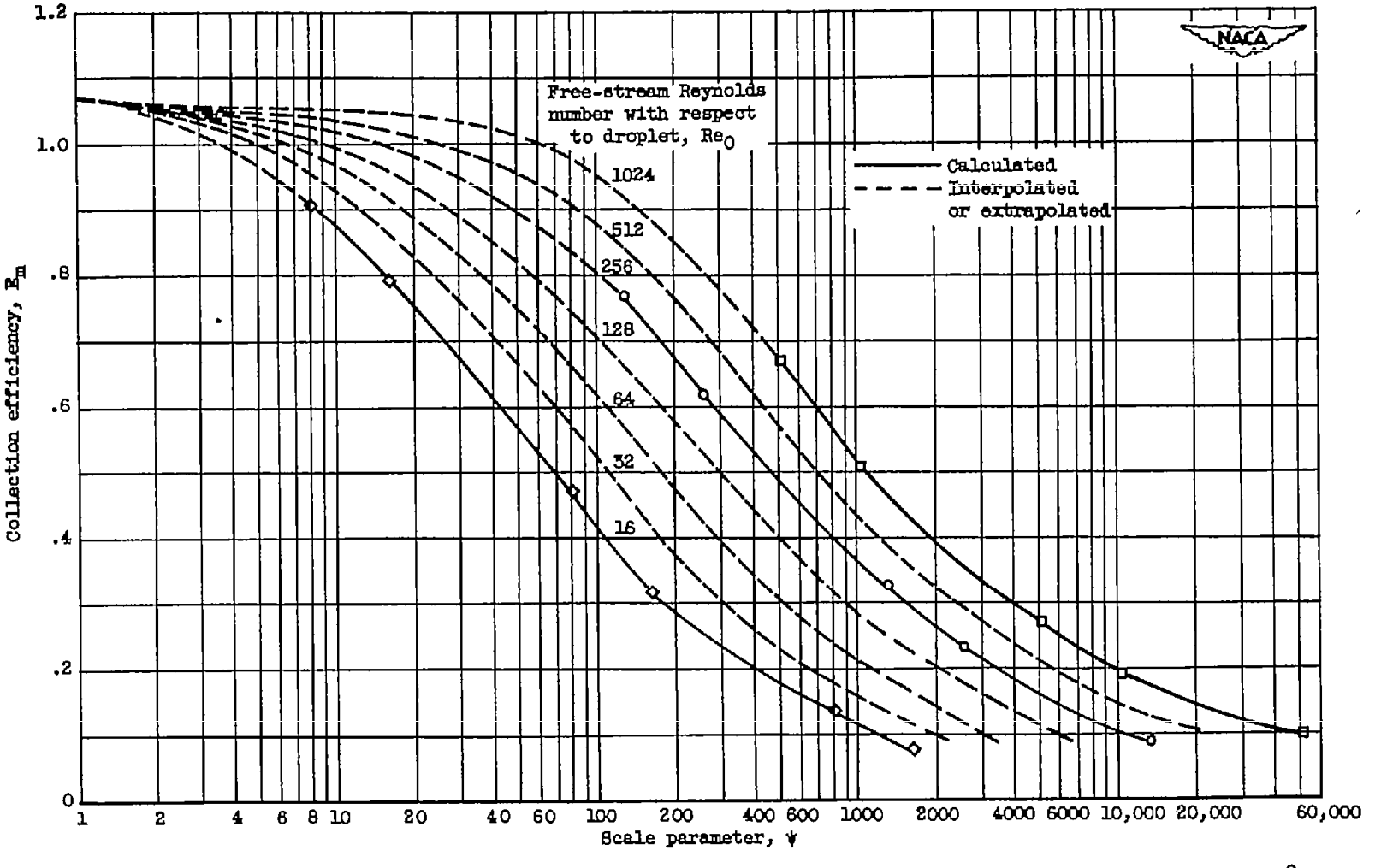

Figure 7. - Collection efficiency of NACA 65_1-212 airfoil as function of scale parameter. Angle of attack, 4°. (Reproduced from fig. 4, ref. 2.)

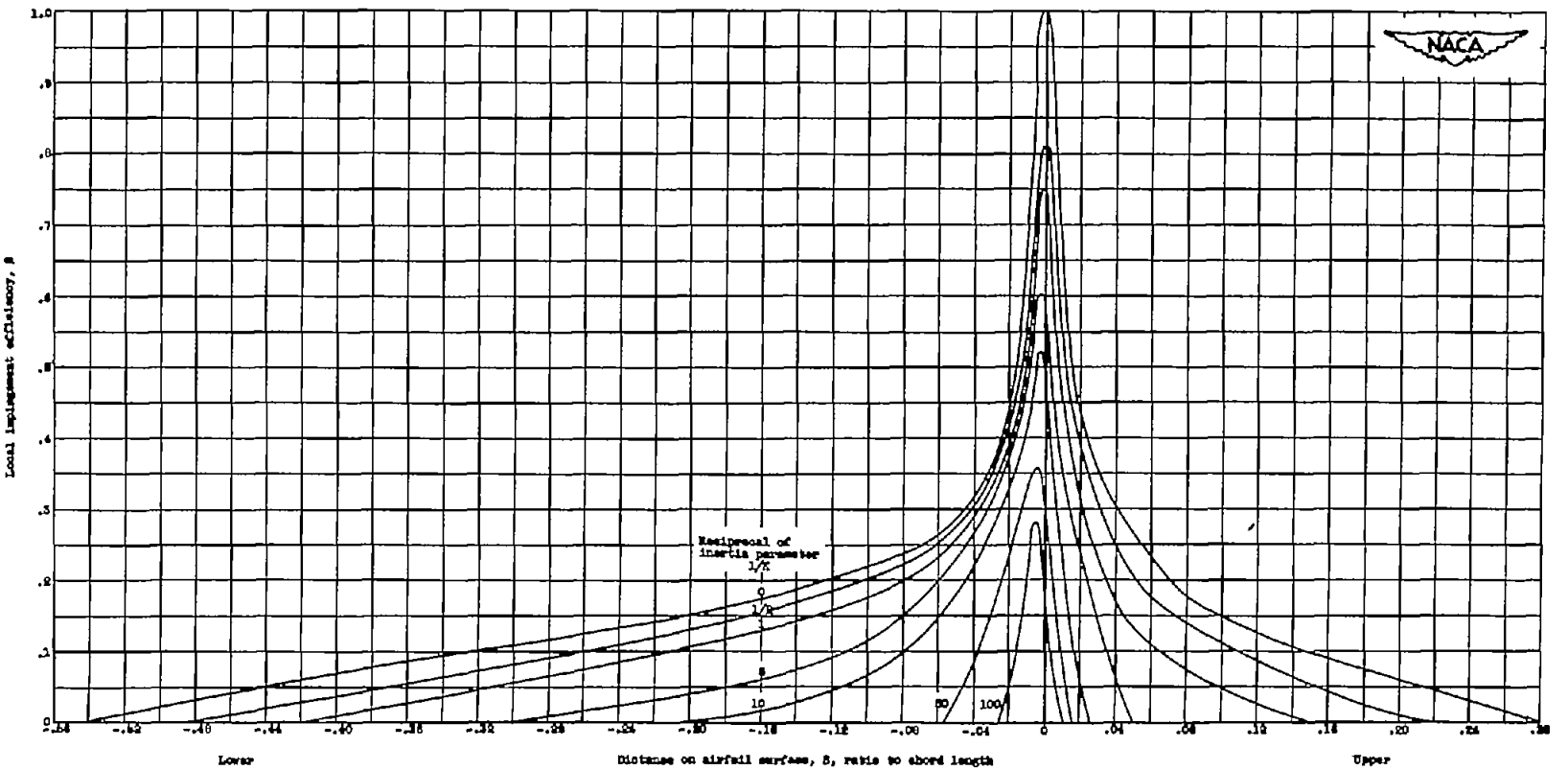

(a) Free-stream Reynolds number with respect to droplet, 15.

Figure 8. - Local impingement efficiency. NACA 65$_1$-212 airfoil; angle of attack, 4°. (Reproduced from fig. 10, ref. 8.)

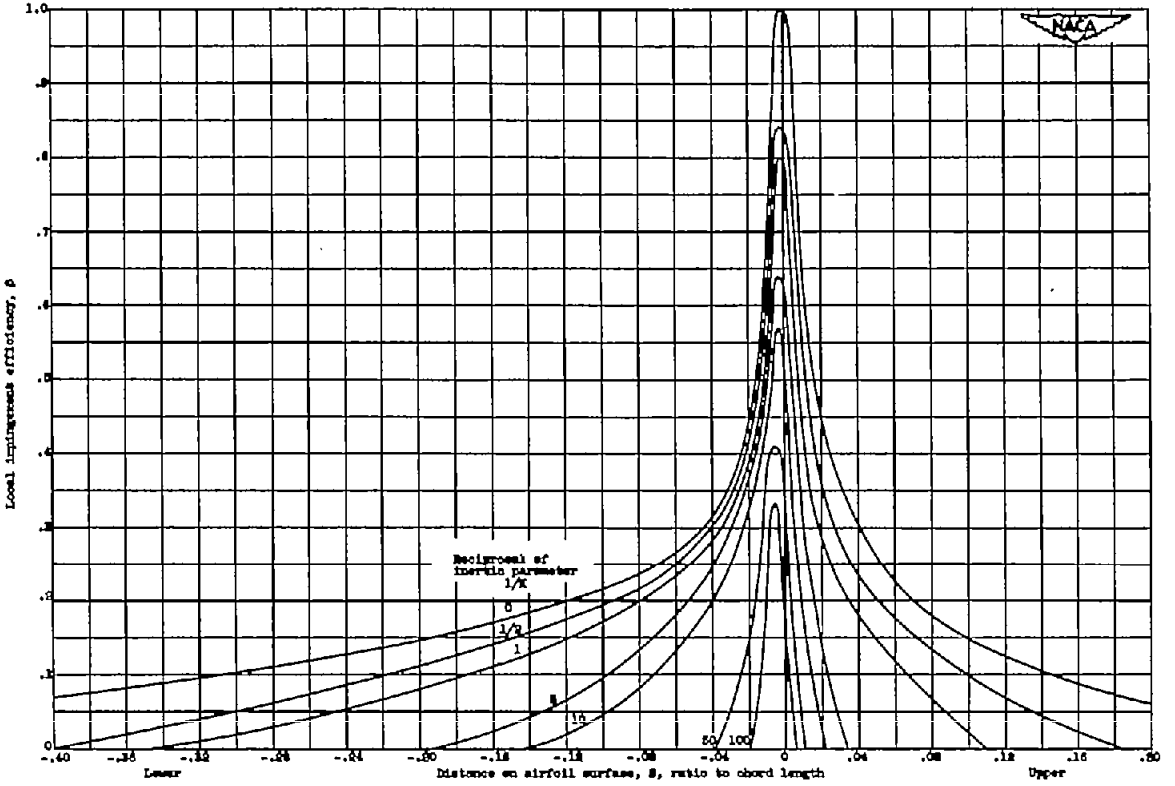

(b) Free-stream Reynolds number with respect to droplet, 258.

Figure 8. - Continued. Local impingement efficiency. NACA 65_1-212 airfoil; angle of attack, 4°. (Reproduced from fig. 10, ref. 2.)

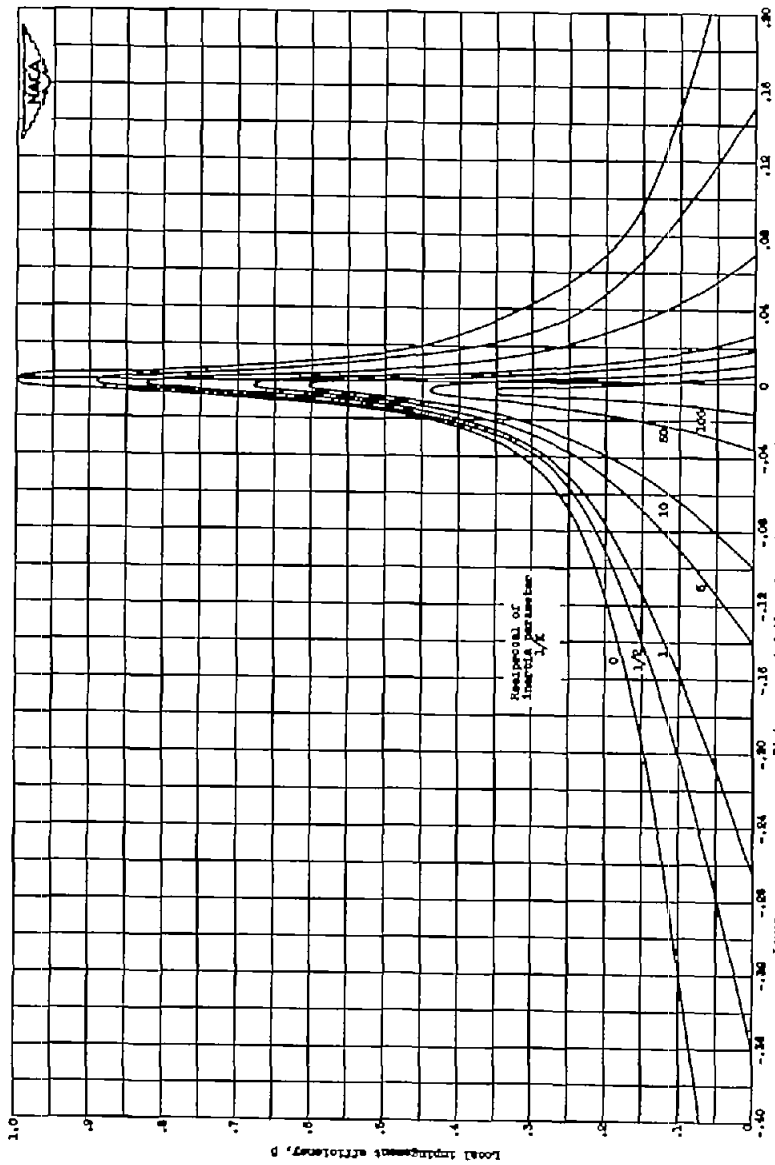

(e) Free-stream Reynolds number with respect to droplet, 1024.

Figure 6. - Concluded. Local impingement efficiency. NACA 65$_1$-212 airfoil; angle of attack, 4°. (Reproduced from fig. 10, ref. 2.)